




Asymmetry in the Length Scales of the Solar Supergranulation Network

K. P. Raju 

Indian Institute of Astrophysics, Bangalore 560034, India; kpr@iia.res.in

Received 2020 February 19; revised 2020 August 1; accepted 2020 August 4; published 2020 August 20

Abstract

Supergranulation is the horizontal velocity pattern on the solar surface with a typical size of 30,000 km and a lifetime of 24 hr. The network structure seen in chromospheric lines, such as Ca II K 3934 Å, is the manifestation of supergranulation. The network seen in the extreme-ultraviolet lines like He II 304 Å is the extension of the chromospheric network into the upper solar atmosphere. We have obtained the length scales of the supergranulation network from the autocorrelation function of calcium II K spectroheliograms from the Kodaikanal archival data. The behavior of the length scales in the horizontal (parallel to the direction of rotation) and vertical (perpendicular to the direction of rotation) have been obtained in different latitudes for a period of about 100 yr. The time-averaged length scales show a nearly symmetric variation in the northern and southern hemispheres. The length scales also show a profound asymmetry in the horizontal and vertical directions, which is dependent on solar latitude. A comparison reveals that both length scales are almost equal near the equatorial latitudes, but the vertical length scales relatively become smaller toward higher latitudes. The asymmetry is independently verified from He II 304 Å images from the Solar Dynamic Observatory/Atmospheric Imaging Assembly. As the length scales are related to the width of the network, the results point to the asymmetry in the supergranular cell boundary. Supergranulation is one of the basic length scales of solar convection, hence these results can have implications for the convection in Sun-like stars.

Unified Astronomy Thesaurus concepts: [Solar atmosphere \(1477\)](#); [Solar cycle \(1487\)](#); [Solar chromosphere \(1479\)](#)

1. Introduction

The bright emission network in the chromospheric Ca II lines has been known since the end of the nineteenth century, soon after the invention of spectroheliograph by Hale and Deslandres, but it remained a mystery for several decades. Velocity measurements over the solar disk revealed a cellular pattern only much later (Hart 1954). In the early 1960s the network was explained on the basis of large-scale solar convection known as the supergranulation, which sweeps the magnetic flux elements to cell boundaries (Leighton et al. 1962; Simon & Leighton 1964). However, the origin of supergranulation, as well as its relation to the magnetic field and the solar dynamo, are still under active investigation (Meunier et al. 2008; Rieutord & Rincon 2010). More recent findings, such as the wave-like properties of supergranules (related to its super-rotation), also support these investigations (Gizon et al. 2003).

The extreme-ultraviolet (EUV) observations from Skylab during 1973–74 have shown that the chromospheric network extends to the transition region (Reeves et al. 1974; Reeves 1976). The network contrast was found to increase with the atmospheric height, and the maximum was reported in the mid-transition region at about $\log T = 5.4$ (Gallagher et al. 1998). The network fades and slowly disintegrates at coronal heights.

The length scales of the supergranulation network are usually obtained from the autocorrelation function of Ca II K images, magnetograms, or Dopplergrams (Simon & Leighton 1964; Singh & Bappu 1981; Wang et al. 1996; Hagenaar et al. 1997; Gontikakis et al. 2003). The halfwidth of the autocorrelation function gives the length scale of supergranulation, which is related to the width of the network boundary (Patsourakos et al. 1999; Tian et al. 2008). The separation between the primary and the secondary peaks gives

the size of the supergranules (Simon & Leighton 1964). We have considered only the former in the present analysis as the secondary peak of the autocorrelation function is not always easily observable. However, it may also be noted that the halfwidth is affected by the data smoothing involved (Srikanth et al. 2000).

The measurements made using an autocorrelation device on Ca II K spectroheliograms had shown (Sýkora 1970) that the length scales and sizes of supergranules are lengthened in the direction of the solar rotation as compared to the perpendicular direction. Also, this flattening was found to fade out with magnetic activity. Large asymmetry in the length scales of the transition region images from the SOLar and Heliospheric Observatory (SOHO)/Coronal Diagnostic Spectrometer (CDS; Harrison et al. 1995) observations was reported, which was attributed to instrumental effects (Raju 2016). In the present work, this asymmetry is examined in more detail, both in latitude and time. We have primarily used calcium II K spectroheliograms from Kodaikanal archival data. The He II 304 Å images from Solar Dynamic Observatory (SDO)/Atmospheric Imaging Assembly (AIA; Lemen et al. 2012) were also used to verify the results.

2. Results

The present work deals with the length scales from the equatorial to the high-latitude regions, hence the impacts of foreshortening effects need to be evaluated. Assuming that the network characteristics do not change significantly during a three minute period, we have selected fifteen AIA 304 Å images with a cadence of 12 s and solar $B_0 = -7^\circ$. It may be noted that when $B_0 = \pm 7^\circ$, the central window is displaced maximum from the disk center. From each image, square windows of size 200 (pixel)^2 ($120 \times 120 \text{ (arcsec)}^2$) were taken in the central meridian from 60° N to 60° S with an interval of

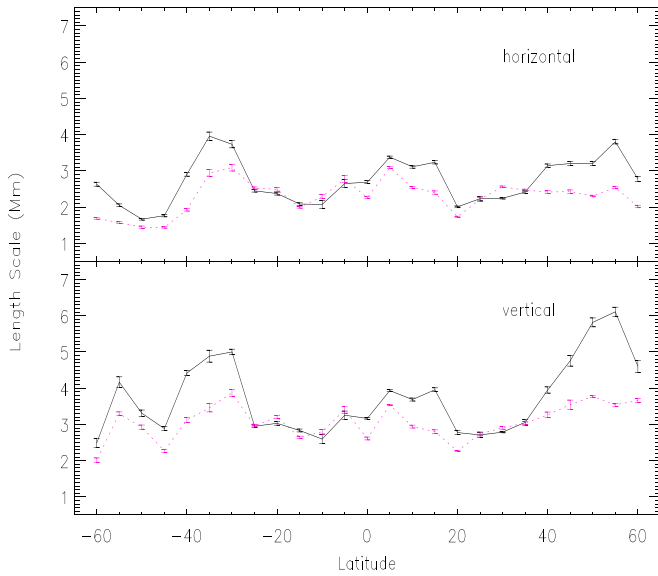


Figure 1. Impacts of foreshortening effect from SDO/AIA data. The upper panel shows the horizontal length scales and the lower panel shows the vertical length scales. The solid line represents the length scales where foreshortening is not considered. The dashed line represents length scales where foreshortening is taken into account. The error bars represent the standard deviation in the measurement.

5° . The two-dimensional autocorrelation function as a function of lag was calculated from the windows. The halfwidth of the autocorrelation function was obtained in the horizontal and vertical directions. The values were corrected for the instrumental point-spread function (PSF; Boerner et al. 2012). The process was repeated for 15 images and the mean and the standard deviation of the horizontal and vertical length scales were obtained. The standard deviation gives an independent measure of the error estimate for the AIA data.

Calculations using the solar coordinate system show that a 200×200 (pixel) 2 window at the solar center will correspond to a 7.2×7.2 (deg) 2 in the solar latitude and longitude. Considering the mapping on the solar sphere, the same window will correspond to 14×14 (deg) 2 at 60° latitude. Keeping the same angular coverage as of the central window, we have calculated the projected area at each latitude and obtained the length scales. The length scales and the error estimates are plotted in Figure 1 along with the corresponding values obtained above where projection effects are not taken into account. It can be seen that the foreshortening is significant, especially at the higher latitudes, and cannot be neglected.

The calcium II K spectroheliograms from the Kodaikanal Solar Observatory cover a period of about 100 yr from 1907. They have a spatial resolution of about $2''$ (Bappu 1967) and are available in a digitized $4K \times 4K$ format with a pixel size of $0''.86$. We have selected about 34,000 spectroheliograms for the analysis. From each spectroheliogram, square windows of size 120 (arcsec) 2 were taken, corrected for foreshortening, and the length scales were obtained as above. The Kodaikanal instrument has a theoretical PSF of only $0''.3$ and the images are dominated by the atmospheric seeing. The length scales were found to have a clear dependence on the solar cycle and the annual variations. The annual variations were removed by averaging the length scales over a year, which enable us to see the long-term tendencies clearly. The results are shown in Figure 2 where the horizontal and vertical length scales are

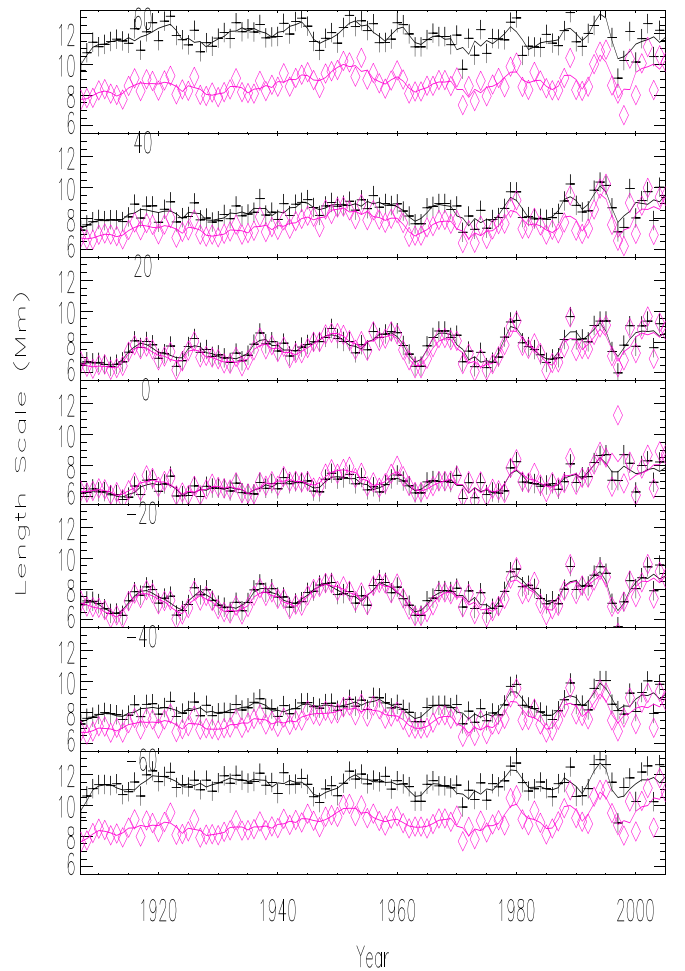


Figure 2. Variation of horizontal and vertical length scales against time from Kodaikanal data. Panels represent different latitudes. Crosses represent horizontal length scales and diamonds represent vertical length scales. The continuous line is a three-point running average.

plotted against time for different latitudes. For clarity, only seven representative latitudes are shown in the figure.

The difference between the horizontal and vertical length scales is about 3 Mm at 60° latitude, which is more than double the spatial resolution of the data (1.45 Mm). However, at 40° latitude, the difference is only 1 Mm, which is less than the spatial resolution, but the difference is consistent over a period of 100 yr. Similar behavior is found near the equatorial latitudes, although the difference is much lesser.

Figure 2 shows that the temporal variation of the yearly averaged length scales has a dependence on the solar cycle that is more pronounced in the sunspot latitudes. We can see the variations due to 10 solar cycles in the data. The dependence of length scales on the solar cycle was reported earlier (Raju 2018). The length scales show a systematic increase during the observational period. There are very few studies on the long-term variation of the spatial resolution of the Kodaikanal data. A recent study of the atmospheric seeing at Kodaikanal during 2017 January–April gives an average value of $2''.6$ (Sridharan 2016–17). The instrument set-up used was the same throughout the 100-year period and no degradation has been reported, although it cannot be ruled out. As noted above, the instrument PSF is only a fraction of the atmospheric seeing, and hence the secular increase in widths could be mostly due to the deterioration of atmospheric seeing with

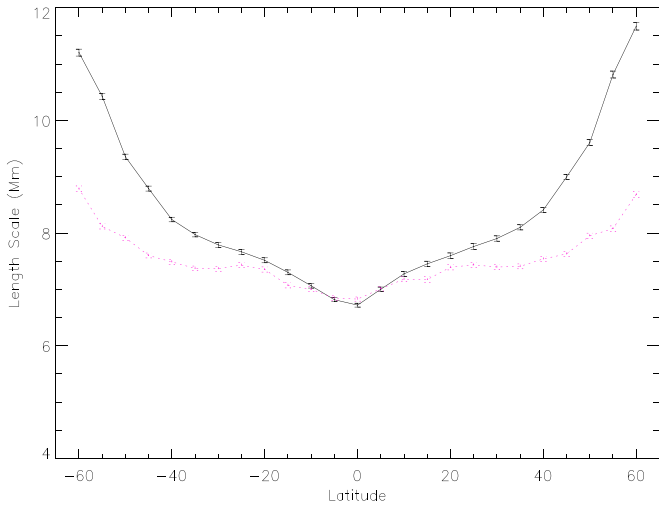


Figure 3. Variation of the time-averaged horizontal and vertical length scales against latitude from Kodaikanal data. The black line represents horizontal length scales and the pink line represents vertical length scales.

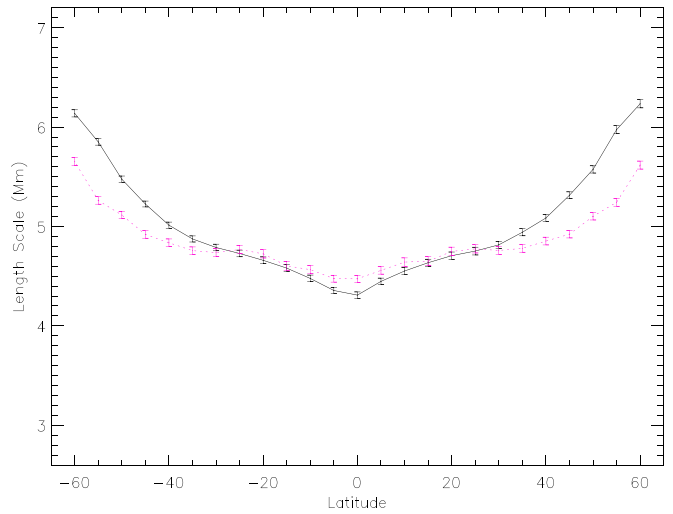


Figure 4. Variation of the time-averaged horizontal and vertical length scales obtained from the one-dimensional autocorrelation function plotted against latitude from Kodaikanal data. The line pattern remains the same as in Figure 3.

time. A reduction in spatial resolution is equivalent to the smoothing of the data, which is known to increase the length scales (Srikanth et al. 2000). The length scales also show an interesting dependence on solar latitude, which is different for the two cases.

In order to see the mean variation of length scales with solar latitude, we have averaged the data in time, which is shown in Figure 3. The given error bars are the standard error of the mean. It can be seen that both horizontal and vertical length scales show a nearly symmetric variation in the northern and southern hemispheres. The length scales show a peak at about $\pm 20^\circ$ latitude and a dip close to the equator. It can be seen that the length scales show a profound asymmetry in the horizontal and vertical directions, which is dependent on solar latitude. A comparison reveals that both length scales are almost equal near the equatorial latitudes but the vertical length scales relatively become smaller toward higher latitudes. The length scales show a steady increase toward higher latitudes.

The interpretation of the two-dimensional autocorrelation function in the vertical and horizontal directions is somewhat complex due to the contributions from nearby directions (Patsourakos et al. 1999). Hence we have obtained the one-dimensional autocorrelation function where the interpretation is straightforward. For this purpose, we have averaged the three central rows and columns separately from the latitude windows and calculated the one-dimensional autocorrelation function. As above, we have obtained the halfwidth as a function of latitude and time. The result is shown in Figure 4. A comparison with Figure 3 shows that the main features like the peaks at $\pm 20^\circ$ latitude and the central dip are seen here too. The main difference is an overall decrease in the length scales, which can be attributed to the smoothing of nearby directions in the former case.

In order to examine the results from an independent source, we have used He II 304 Å images from SDO/AIA database. The He II line has a peak formation temperature at $\log T = 4.9$ and originates mainly from the chromosphere and the transition region. We have used 672 images during the period 2010–2019. The two-dimensional autocorrelation function was calculated from the latitude windows as above and the length scales were obtained. The temporal variations are

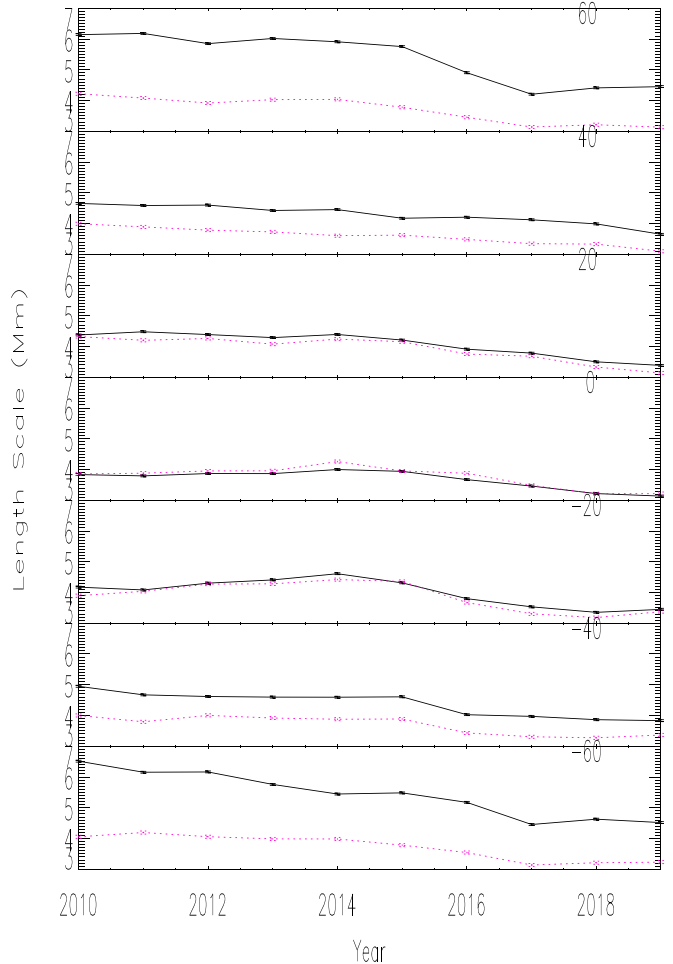


Figure 5. Variation of horizontal and vertical length scales against time from SDO/AIA data. Panels represent different latitudes. The solid line represents horizontal length scales and the dashed line represents vertical length scales.

averaged over one year and the results are shown in Figure 5, where length scales are plotted against time for different latitudes. Solar cycle variations are clearly seen near the equatorial latitudes.

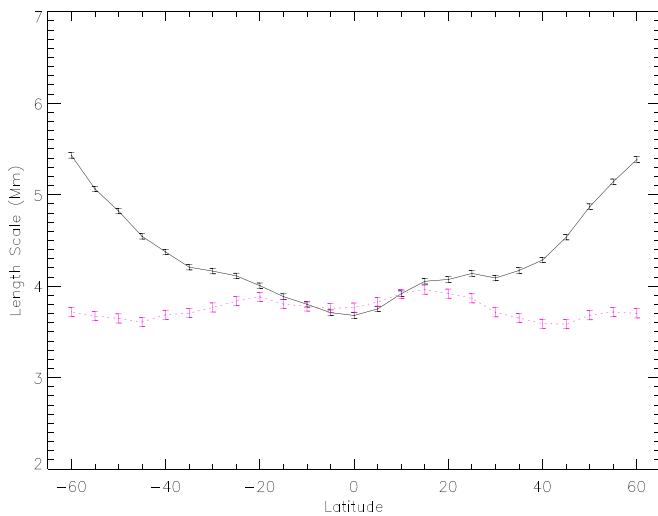


Figure 6. Variation of the time-averaged horizontal and vertical length scales against latitude from SDO/AIA data. The line pattern remains the same as in Figure 3.

The difference between the horizontal and vertical length scales is about 2 Mm at 60° latitude, which is much higher than the spatial resolution (0.54 Mm) of the data. At 20° latitude, the difference is only 0.2 Mm but it is consistent over the period of observation.

The time-averaged length scales are shown in Figure 6. The asymmetry in the horizontal and vertical length scales and its dependence on solar latitude can be clearly seen. A comparison with Figure 3 and 4 shows that the main features such as the central minimum, two local maxima at $\pm 20^\circ$, and a monotonous increase of horizontal length scales toward higher latitudes, are similar in all three figures. The main difference between the two data sets is that the vertical length scales do not show a monotonous increase toward higher latitudes. The reason is not clear, but the two lines originate at different heights and the behavior of length scales could be different at different heights.

The results, in general, do not agree with the earlier finding (Sýkora 1970) that the horizontal length scales are consistently larger than the vertical length scales. The length scales obtained near the equatorial regions show that they are nearly equal. In Raju (2016), vertical length scales in the solar center were found to be larger than the horizontal length scales by 37% and 48% for the transition region lines He I 586 Å and O V 630 Å, respectively, from SOHO/CDS measurements. Hence, the large asymmetry seen in the SOHO/CDS observations is mostly due to the instrumental effects. There are no reports of asymmetric PSFs of the Kodaikanal or AIA instruments. The main features of asymmetry reported from two diverse instruments are similar, hence the possibility of asymmetric PSFs may be ruled out. It can be concluded that the horizontal and the vertical length scales are, in general, different and they have a clear dependence on solar latitude.

The length scale of the supergranulation network is related to the width of the network boundary, therefore it can be concluded that the width of the network boundary lacks circular symmetry. This is the first time that the asymmetry in the supergranular boundary width and its dependence on solar latitude is being reported extensively. It may be noted that the pole-equator difference of supergranular sizes and their dependence on directions have been reported (Muenzer et al.

1989). Also, a north–south alignment of the supergranulation was pointed out previously (Lisle et al. 2004). The dependence of asymmetry on solar latitude suggests that factors such as differential rotation, meridional circulation, torsional oscillations, and local magnetic fields play a role. Because supergranulation is one of the basic length scales of solar convection, these results can have implications for the convection in Sun-like stars.

3. Conclusions

The horizontal and vertical length scales of the supergranulation network were obtained from the calcium II K spectroheliograms from 1907 to 2007 from the Kodaikanal archival data. Both the length scales show a dependence on the solar cycle that is more pronounced in the sunspot latitudes. The time-averaged length scales show a nearly symmetric variation in the northern and southern hemispheres. A comparison of the two length scales show a profound asymmetry dependent on solar latitude. Both length scales are almost equal near the equatorial latitudes, but the vertical length scales become relatively smaller toward higher latitudes. The asymmetry in the length scales has been verified from the one-dimensional autocorrelation function obtained from the same observational windows. The He II 304 Å images from the SDO/AIA database were also used in the analysis, and it was found that the asymmetry in the length scales is seen here as well. A comparison of the two data sets shows that the main features, such as the central minimum, two local maxima at $\pm 20^\circ$ and a monotonous increase of horizontal length scales toward higher latitudes, are similar. The main difference is that the vertical length scales from AIA do not show a monotonous increase toward higher latitudes. The behavior of the horizontal and vertical length scales points to the asymmetry in the supergranular boundary width and its dependence on solar latitude, which is reported for the first time here. The implications of these results on the solar and stellar convection need to be examined. The recently launched Solar Orbiter mission (Müller et al. 2013, 2020) will provide solar images with unprecedented surface details from high latitudes. The data will be useful for studying further the asymmetry in the supergranular length scales reported here.

This work was funded by the Department of Science and Technology, Government of India. The author would like to thank Prof. Jagdev Singh and the digitization team of the Indian Institute of Astrophysics. Kodaikanal Solar Observatory is a facility of Indian Institute of Astrophysics, Bangalore, India. This data is now available for public use at <http://kso.iiap.res.in> through a service developed at IUCAA under the Data-Driven Initiatives project funded by the National Knowledge Network. The AIA data are courtesy of SDO (NASA) and the AIA consortium.

ORCID iDs

K. P. Raju  <https://orcid.org/0000-0002-6648-4170>

References

- Bappu, M. K. V. 1967, *SoPh*, **1**, 151
- Boerner, P., Edwards, C., Lemen, J., et al. 2012, *SoPh*, **275**, 41
- Gallagher, P. T., Phillips, K. J. H., Harra-Murnion, L. K., & Keenan, F. P. 1998, *A&A*, **335**, 733
- Gizon, L., Duvall, T. L., & Schou, J. 2003, *Natur*, **421**, 43

- Gontikakis, C., Peter, H., & Dara, H. C. 2003, *A&A*, 408, 743
- Hagenaar, H. J., Schrijver, C. J., & Title, A. M. 1997, *ApJ*, 481, 988
- Harrison, R. A., Sawyer, E. C., Carter, M. K., et al. 1995, *SoPh*, 162, 233
- Hart, A. B. 1954, *MNRAS*, 114, 17
- Leighton, R. B., Noyes, R. W., & Simon, G. W. 1962, *ApJ*, 135, 474
- Lemen, J. R., Title, A. M., Akin, D. J., et al. 2012, *SoPh*, 275, 17
- Lisle, J. P., Rast, M. P., & Toomre, J. 2004, *ApJ*, 608, 1167
- Meunier, N., Roudier, T., & Rieutord, M. 2008, *A&A*, 488, 1109
- Muenzer, H., Schroeter, E. H., Woehl, H., & Hanslmeier, A. 1989, *A&A*, 213, 431
- Müller, D., Marsden, R. G., St., Cyr, O. C., et al. 2013, *SoPh*, 285, 25
- Müller, D., Zouganelis, I., St., Cyr, O. C., et al. 2020, *NatAs*, 4, 205
- Patsourakos, S., Vial, J. C., Gabriel, A. H., & Bellamine, N. 1999, *ApJ*, 522, 540
- Raju, K. P. 2016, *SoPh*, 291, 3519
- Raju, K. P. 2018, *MNRAS*, 478, 5056
- Reeves, E. M. 1976, *SoPh*, 46, 53
- Reeves, E. M., Foukal, P. V., Huber, M. C. E., et al. 1974, *ApJL*, 188, L27
- Rieutord, M., & Rincon, F. 2010, *LRSP*, 7, 2
- Simon, G. W., & Leighton, R. B. 1964, *ApJ*, 140, 1120
- Singh, J., & Bappu, M. K. V. 1981, *SoPh*, 71, 161
- Sridharan, R. 2016-17, IIA Annual Report 30
- Srikanth, R., Singh, J., & Raju, K. P. 2000, *ApJ*, 534, 1008
- Sýkora, J. 1970, *SoPh*, 13, 292
- Tian, H., Marsch, E., Tu, C. Y., Xia, L. D., & He, J. S. 2008, *A&A*, 482, 267
- Wang, H., Tang, F., Zirin, H., & Wang, J. 1996, *SoPh*, 165, 223